Optical properties of $YBa_2Cu_3O_{7-\delta}$ and $PrBa_2Cu_3O_{7-\delta}$ films: High-energy correlations and metallicity

J. Bäckström,* D. Budelmann,† R. Rauer, and M. Rübhausen
Institut für Angewandte Physik, Universität Hamburg, Jungiusstraße 11, D-20355 Hamburg, Germany

H. Rodríguez and H. Adrian
Institut für Physik, Universität Mainz, D-55099 Mainz, Germany

(Received 8 December 2003; revised manuscript received 7 April 2004; published 4 November 2004)

We have investigated the temperature dependence of the dielectric functions of a high-T_c superconducting $YBa_2Cu_3O_{7-\delta}$ (Y-123) and a nonsuperconducting $PrBa_2Cu_3O_{7-\delta}$ (Pr-123) thin film using spectral ellipsometry. We evaluate the data by means of thermal-difference and sum-rule analysis techniques. We find that a spectral-weight transfer into the bands between 4 and 5 eV takes place before Y-123 becomes superconducting. We identify an anomaly around 1 eV that can be explained by a sudden plasma-frequency drop of the order of an meV around T_c. The absence of any sudden effects in the dielectric properties of Pr-123 suggests that both observations are intimately related to the superconducting state. Our findings point out that high-energy degrees of freedom must be considered for the understanding of high-temperature superconductivity.

DOI: 10.1103/PhysRevB.70.174502 PACS number(s): 74.72.−h, 74.78.Bz, 74.25.Gz, 74.25.Jb

I. INTRODUCTION

The cuprates belong to the strongly correlated transition-metal oxides. Such materials are characterized by intriguing interplays between different degrees of freedom and their properties are rooted in physics on both low- (around k_BT) and high- (well above k_BT) energy scales. These characteristics make the nature of the materials difficult to understand and many questions remain open. One example in the field of high-temperature superconductivity is the unresolved disappearance of superconductivity when Pr is substituted into the Y-based cuprates.[1] Other rare-earth substitutions yield materials with essentially unchanged superconducting properties. Different ideas have been proposed to explain this effect, including hole filling by Pr^{4+},[2] hybridization of Pr $4f$ and O $2p$ orbitals leading to charge localization,[3] as well as presence of Pr on the Ba site.[4] Experimental support for the Pr $4f$ – O $2p$ hybridization scenario exists,[5] as well as challenges.[6] The situation is complicated by some reported observations of superconductivity in $PrBa_2Cu_3O_7$ (Pr-123) prepared under special conditions.[7,8]

$YBa_2Cu_3O_7$ (Y-123) is a well-studied member of the family of cuprate superconductors with a T_c of up to 93.6 K.[9] Pr-123, on the other hand, is a long-range ordered antiferromagnet below $T_N \approx 280$ K.[10] Recent Raman scattering studies on superlattices of alternating Y-123 and Pr-123 layers have revealed that the Pr-123 layer responds to the onset of superconductivity in the Y-123 layer through the proximity effect, manifested by phonon,[11] two-magnon, and electron[12] spectra.

A growing set of evidence points out that the properties of cuprate superconductors are not governed by mechanisms living at energies close to the Fermi level alone. Recently, Stanescu and Phillips introduced the term "Mottness" in a theory demonstrating that spectral-weight transfer between low and high energies is an intrinsic property of a doped Mott-Hubbard insulator, when strong local correlations are considered.[13,14] Several spectroscopy studies have seen peculiar effects taking place around T_c at surprisingly high energies, in the mid-infrared to visible range.[15–22] The nonsuperconducting Pr-123 and the superconductor Y-123 are structurally very similar. Thus, it is of interest to investigate and compare their high-energy excitation spectra.

Spectroscopic ellipsometry is a powerful tool for investigations of electronic properties of solids. By analyzing the change in the polarization state of light reflected from a sample surface, the real and imaginary components of the dielectric function can be extracted without applying numerical Kramers-Kronig analysis.[23] The technique has thus a high accuracy.

In this paper, we present the temperature dependence of the dielectric function of Y-123 and Pr-123 thin films measured with ellipsometry between 0.5 and 5.0 eV. We show that the dielectric functions of Y-123 and Pr-123 are rather similar, with the most notable difference being a metallic response at lower frequencies existing in Y-123 but not in Pr-123. We analyze the temperature dependence by means of traditional sum-rule techniques as well as the innovative temperature-differential method introduced by Holcomb *et al.*[15,16] It is found that a spectral-weight transfer into the bands between 3.9 and 4.8 eV preceeds the superconducting transition in Y-123. Furthermore, we find that a T_c-induced anomaly around 1 eV in the real part of the dielectric function can be satisfactorally explained by the Drude model assuming a sudden plasma-frequency decrease of the order of an meV. However, other anomalies present above 4 eV cannot be described by this model. The absence of any such sudden anomalies in Pr-123 suggests that both effects are intimately connected to superconductivity. The results give additional evidence that the physics of high-temperature superconducting cuprates is governed by interplays between degrees of freedom living on very different energy scales, from around the Fermi level up to several eV.

II. EXPERIMENTAL

We produced *c*-axis oriented Y-123 ($T_c \approx 89$ K) and Pr-123 films on $SrTiO_3(100)$ substrates using a multi-target dc sputtering system.[24] The substrate temperature was 1115 K and the atmosphere was a 2:1 mixture of argon and oxygen with a total pressure of 3 mbar. The layer thicknesses of about 300 nm were controlled by the sputtering time. We found deposition rates to be 20 Å/min and 27 Å/min for Y-123 and Pr-123, respectively. The film sizes were 0.5×0.5 cm^2. Sample characterization by means of x-ray diffraction and Raman spectroscopy reveals excellent (001) surfaces. Ellipsometry characterization measurements at room temperature for different angles of incidence verifies the bulk behavior of the films and that the *c*-axis influence on the measurement is negligible. Furthermore, measurements with different planes of incidence relative to the sample orientation show very small deviations, demonstrating that the samples are finely twinned on the scale of the incident light spot and can be considered as isotropic also in the a/b plane. Thus, the ellipsometric angles Ψ and Δ were converted to the dielectric function $\epsilon_r = \epsilon_1 + i\epsilon_2$ assuming an isotropic, infinitely thick sample.[23] This dielectric function is the dielectric tensor component for light polarized parallel to the cuprate planes that is the average of $\boldsymbol{E} \| a$ and $\boldsymbol{E} \| b$.

The experiments have been performed using an extended Sentech SE850 spectral ellipsometer equipped for a spectral range from 0.5 to 5.5 eV. As light sources we use a high-pressure Xe-discharge lamp (ultraviolet-visible) and a halogen lamp (near infrared). In the visible spectral range, the spectral resolution is achieved with a single-grating spectrograph equipped with a diode-array detector. In the near-infrared range we make use of a Fourier-transform spectrometer. We mounted the films into a CryoVac He-flow cryostat on pieces of sandblasted silicon in order to avoid unwanted signal reflected by the coldfinger. The angle of incidence, restricted by the geometry of the cryostat, was kept at 70°. The optical windows of the cryostat are stress free and have a negligible influence on the polarization state of the light. The base pressure of this system was about 1×10^{-8} mbar at room temperature. Since ellipsometric measurements are very sensitive to even very small freeze-outs on the sample surface, we employed a measurement protocol with thermal cyclings between 10 K and room temperature between each pair of measured temperature points.

III. RESULTS AND DISCUSSION

The complex dielectric functions for Y-123 and Pr-123 are shown in Fig. 1 for several temperatures. For photon energies between 0.5 and 2 eV we observe a typical metallic response in Y-123, as signaled both by a zero crossing of ϵ_1 [Fig. 1(a)] and a rapidly increasing ϵ_2 [Fig. 1(b)] with decreasing frequency. Pr-123 shows no such zero-crossing [Fig. 1(c)], but still an ϵ_2 increase towards lower frequencies [Fig. 1(d)]. This increase of ϵ_2 in Pr-123 towards lower energies can be due to interband transitions at finite energies below 0.8 eV, and/or a weak metallic response from the CuO chains.[25,26]

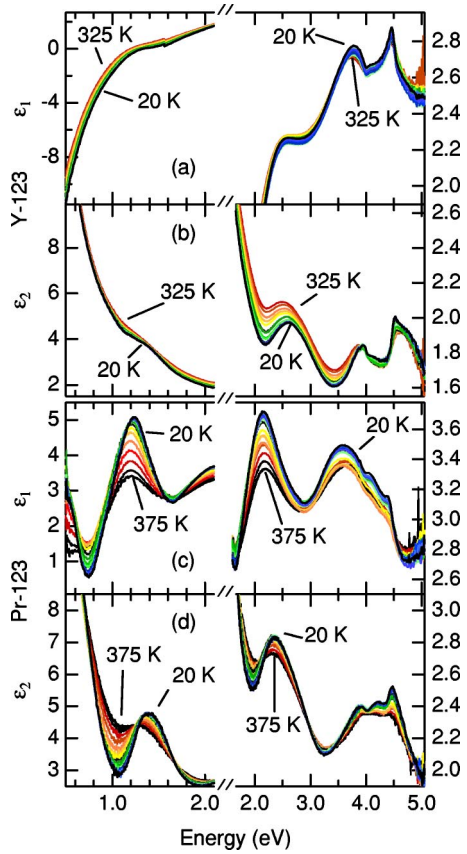

FIG. 1. (Color online) Real and the imaginary parts of the dielectric function for Y-123 (a,b) and Pr-123 (c,d) for selected temperatures. The panels are split into low- and high-energy parts for clarity.

Cooling down Pr-123 from 350 K to 200 K, i.e., through the Néel temperature $T_N \approx 280$ K,[10] we observe a peak shifting from 1.3 to 1.4 eV, sharpening, and gaining strength, see Fig. 1(d). Below 200 K this peak shows no further significant changes. A peak at about the same resonance energy showing a similar sharpening with decreasing temperature can be seen also in the Y-123 spectra [Fig. 1(b)], although significantly weaker and partly buried in the Drude response. The 1.4-eV peak has been attributed to a charge-transfer (CT) excitation, O $2p \rightarrow$ Cu $3d$, in the CuO_2 planes.[25]

The right panels of Fig. 1 show ϵ_r for the visible-ultraviolet region. Y-123 and Pr-123 are exhibiting excitation peaks at similar energies in ϵ_2 [panels (b) and (d), respectively]. At 2.6 eV, ϵ_2 of Y-123 shows a strong peak that sharpens and hardens as the temperature is lowered. A peak at 2.3 eV in Pr-123 displays an analog temperature evolution. Kircher *et al.* assigned a peak in the component along the *a* axis of the dielectric function at around this energy to an excitation into the antibonding Cu(2)–O(2)–O(3) band, with the initial state being found in a manifold of strongly dispersive bands.[27]

At higher energies, both compounds show a complicated structure of overlapping peaks between ~3.5 and 5 eV. We discuss the Pr-123 sample first. Here, three peaks can be resolved by inspection of the low-temperature data, namely around 3.9, 4.3, and 4.5 eV. At higher temperatures, the three

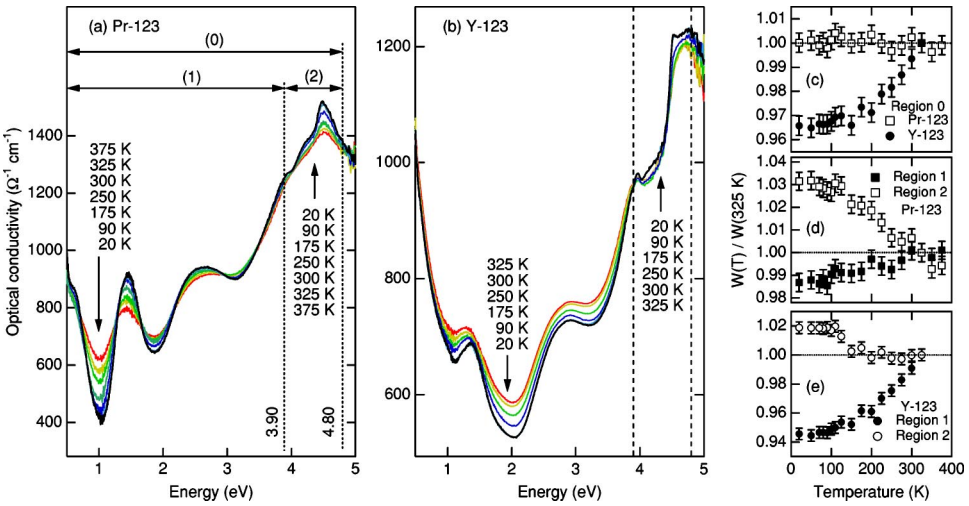

FIG. 2. (Color online) Real part of the optical conductivity ($\sigma_1=\omega\epsilon_0\epsilon_2$) at selected temperatures over the whole measured spectral range for Pr-123 (a) and Y-123 (b). The integration ranges used for the sum-rule analysis are marked and labeled. The three panels on the right show normalized integrated optical conductivity for Y-123 and Pr-123 as indicated. (c) shows the integration over region 0 for both compounds, (d) and (e) show the integrals over regions 1 and 2 for Pr-123 and Y-123, respectively.

peaks are broad and somewhat weaker. At the highest temperatures the peaks float together and the ϵ_2 curve forms an almost flat plateau between 3.9 and 4.5 eV. Y-123 shows peaks at similar energies, but the peak at 4.1 eV is significantly weaker. In fact, it is hardly visible for temperatures above ~110 K. The 3.9-eV peak sharpens and hardens as the temperature is lowered. At high temperatures, we find a peak around 4.5 eV in Y-123, reminiscent to the situation in Pr-123. However, below ~150 K, when the peaks sharpen, it becomes evident that this structure consists of two peaks, one fairly broad centered around 4.64 eV and one really sharp peak at 4.52 eV.

The peak at 4.1 eV has been reported to be very sensitive to oxygen deficiency and to chain-oxygen ordering.[27–29] It has been assigned to intra-ionic excitations in chain-layer Cu of the character $3d_{3z^2-r^2}\rightarrow 4p_x$, also involving to a minor extent Cu $3d_{3z^2-r^2}\rightarrow$ Ba charge transfer,[30] but also to a CT transition within the O–Cu–O "dumbbell" of chain Cu and apical O,[31] as well as a Ba–O CT excitation.[29] Preliminary resonant-Raman data on Y-123 single crystals measured in our group show a strong enhancement of the Ba phonon-mode intensity for excitation energies around 4.1 eV, in support of the involvement of Ba orbitals in the 4.1-eV excitation.

A. Sum-rule analysis

To discuss the changes of the spectra with temperature, it is useful to look at the optical conductivity σ rather than the dielectric function, since the real part of σ is proportional to the effective charge-carrier concentration and should obey the sum rule. Therefore, changes in the optical conductivity provide a picture of charge-carrier transfers.

The real part of the optical conductivity ($\sigma_1=\omega\epsilon_0\epsilon_2$) is shown for Pr-123 and Y-123 in Figs. 2(a) and 2(b), respectively, for some selected temperatures. It is evident in the comparison between the spectra from Pr-123 and Y-123 that the general shapes of σ_1 are similar. Another similarity is that the high-energy part between 3.9 and 4.8 eV in both compounds displays an increase of spectral weight as the temperature is decreased. Unlike Pr-123, Y-123 shows a spectral-weight loss as the temperature is lowered over the entire frequency range below the isosbestic point at ~3.9 eV.

Figure 2(c) shows the integrated optical conductivity

$$W(T)=\int_{\omega_1}^{\omega_2}\sigma_1(\omega,T)d\omega \qquad (1)$$

over the spectral range between 0.5 and 4.8 eV (region 0) for Pr-123 and Y-123. This panel confirms that the spectral weight drops in the temperature range from 325 K down to 100 K and then stays roughly constant for the superconducting compound, while it remains constant for the nonsuperconducting Pr-123 over the entire measured temperature range. Since Y-123 is known to be metallic, while Pr-123 is an insulator, it is reasonable to assume that the lost Y-123 spectral weight is transferred to the metallic Drude-like response below 0.5 eV, i.e., outside our accessible spectral range.

We can split the spectral region 0 at the isosbestic point of Y-123 at 3.9 eV (which is also close to an isosbestic point of Pr-123), forming regions 1 (0.5—3.9 eV) and 2 (3.9—4.8 eV) [see Fig. 2(a)]. The spectral-weight integrals for these two regions for Pr-123 is shown in Fig. 2(d) and for Y-123 in Fig. 2(e). For Y-123, we see that the spectral weight in region 1 drops with decreasing temperature, with a weak sign of a kink at 120 K. More dramatic is the temperature dependence in region 2. Down to about 120 K, it stays independent of temperature within our accuracy, just to make a sudden increase between 120 and 100 K. Below 100 K, no further changes are observed. Note that the build-up of spectral weight happens before the sample becomes superconducting. This naturally leads to a suspicion that it might be connected to a formation of a pseudogap.

The spectral-weight integrals for Pr-123 are plotted in Fig. 2(d). Region 1 shows a monotonic decrease of spectral weight with decreasing temperature, while region 2 shows an increase. We note that there are some very weak signs of kinks in both curves around 100 K, although they are well within the estimated error bars.

B. Thermal-difference analysis

Holcomb *et al.* measured and analyzed thermal-difference reflectance spectra of several cuprate superconductors.[15,16]

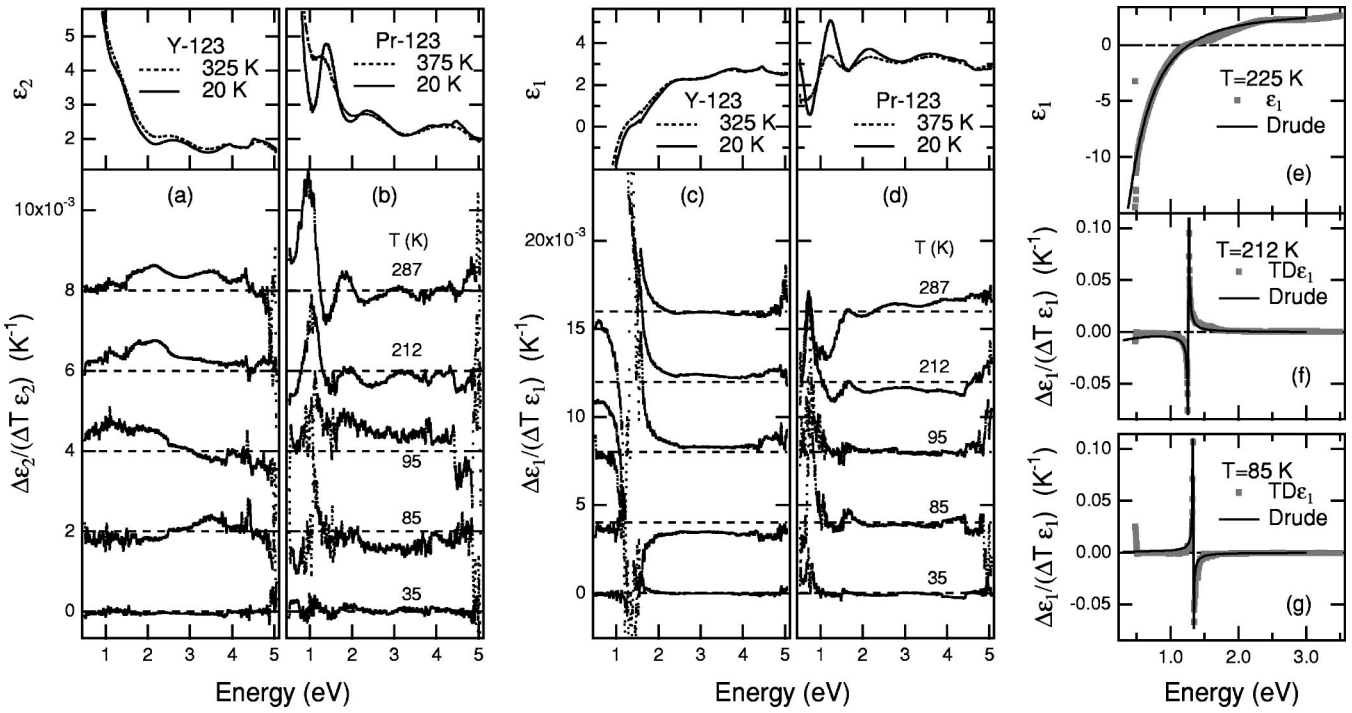

FIG. 3. Normalized temperature-differential spectra of ϵ_2 for Y-123 (a) and Pr-123 (b), ϵ_1 for Y-123 (c) and Pr-123 (d) for a selection of temperatures. The top panels of (a,b,c,d) show the corresponding parts of the dielectric functions for comparison. Panel (e) shows the experimental ϵ_1 for Y-123 at $T=225$ K together with a calculated Drude response, while (f) shows the experimental TDϵ_1 for 212 K together with the modelled Drude response in the normal state. In (g) we show the 85-K TDϵ_1, i.e., the comparison between normal- and superconducting-state properties, together with a calculated Drude TDϵ_1 for a T_c-induced plasma-frequency shift of 0.5 meV.

Investigating the temperature derivative of an entity is a natural approach when looking for temperature-induced changes. Therefore, we calculated the normalized thermal-difference spectra of the dielectric function (TD$\epsilon_{1,2}$) defined as

$$\mathrm{TD}\epsilon_{1,2} = \frac{\Delta\epsilon_{1,2}}{\epsilon_{1,2}\Delta T} = \frac{2[\epsilon_{1,2}(T_2) - \epsilon_{1,2}(T_1)]}{(T_2 - T_1)[\epsilon_{1,2}(T_2) + \epsilon_{1,2}(T_1)]}. \quad (2)$$

The TDϵ_2 spectra for Y-123 are shown in Fig. 3(a). The here noted temperatures are the mean values of the temperature points used to calculate the respective curves. At high temperatures, the relative changes of the dielectric function are not strongly temperature dependent, in agreement with Holcomb *et al.*[15,16] Overall, the temperature derivative of ϵ_2 is positive, consistent with $W(T)$ in Fig. 2(c). Close to the superconducting transition ($T_c \approx 89$ K), the TDϵ_2 shape changes qualitatively, indicating a T_c-induced anomaly in the optical properties. At the lowest temperatures, TDϵ_2 vanishes, in agreement with the constant low-temperature behavior in Figs. 2(c) and 2(e).

The TDϵ_2 spectra for Pr-123 are shown in Fig. 3(b). At high temperatures, we see a strong peak around 1 eV decreasing its strength as the temperature is lowered. This is a result of the sharpening of the 1.4-eV CT excitation, as can be seen by comparison with the top panel. Interestingly, this 1-eV peak is strongest in the 287-K spectrum, i.e., around T_N, indicating that the corresponding excitation is connected to antiferromagnetism. Taken over the whole spectral range, TDϵ_2 assumes both positive and negative values for all temperatures, in consistence with the conserved spectral-weight in Fig. 2(c).

The shape changes of TDϵ_2 for Pr-123 at lower temperature are within the scattering of the data seen when looking at the full temperature dependency. Furthermore, TDϵ_1 for Pr-123 shown in Fig. 3(d) shows no sudden anomalies at all around 90 K. It reflects, though, the T_N-induced anomaly around 1 eV.

The simple temperature dependence of TDϵ_1 of Pr-123 can be contrasted to the data in Fig. 3(c), where we show TDϵ_1 for Y-123. From high temperatures down to slightly above T_c, TDϵ_1 is rather independent of temperature and is close to zero at high frequencies. The clearest feature is the singularity at the zero crossing of ϵ_1. Interestingly, the expected temperature behavior of the simple Drude model, also used by Holcomb *et al.*,[15]

$$\epsilon_1 = \epsilon_\infty - \frac{\omega_p^2}{\omega^2 + \Gamma^2}, \quad (3)$$

$$\frac{\partial \epsilon_1}{\partial T} = \frac{\omega_p^2}{\omega^2 + \Gamma^2}\left(\frac{1}{V}\frac{dV}{dT} + \frac{2\Gamma}{\omega^2 + \Gamma^2}\frac{d\Gamma}{dT}\right), \quad (4)$$

with the typical values $\epsilon_\infty = 3$ as high-frequency dielectric constant, plasma frequency $\omega_p = 1.15$ eV, scattering rate $\Gamma = 0.4$ eV, thermal volume-expansion coefficient $(1/V) \times (dV/dT) = 1.2 \times 10^{-5}\,\mathrm{K}^{-1}$, and $d\Gamma/dT = k_B$, describes the TDϵ_1 (212 K) and ϵ_1 (225 K) surprisingly well, as shown in

Figs. 3(e) and 3(f), respectively. In other words, the high-temperature evolution of ϵ_1 of Y-123 is the expected one for a metal with decreasing scattering and shrinking lattice as the temperature is lowered. In contrast to this, there is a drastic trend change in the TDϵ_1 curves at T_c, with a sign change of the singularity and a nonzero high-energy part. The fact that strong effects around 90 K are seen in Y-123 but not in Pr-123 suggests that they are superconductivity induced. At still lower temperatures, TDϵ_1 is close to zero, indicating that the dielectric function stays essentially independent of temperature. The observed dramatic effect in TDϵ_1 around 1 eV can be reproduced by the Drude model by assuming a negative $d\Gamma/dT$ around T_c in Eq. (4). Alternatively, the effect can be reproduced by a sudden *decrease* of ω_p when the material enters the superconducting state.

Among the two ideas, we find a sudden drop of the plasma frequency more plausible than an increase of the scattering rate. We see no reason why the scattering rate should be higher on the superconducting side of the phase boundary. In fact, the scattering rate should be *reduced* below T_c.[32]

The 85-K spectrum in Fig. 3(c) is compatible with a plasma-frequency drop between 90 and 80 K of the order of 0.5 meV, based on the assumption that the other parameters in Eq. (3), ϵ_∞ and Γ, stay constant. In Fig. 3(g), we show a comparison between the measured TDϵ_1 (85 K) and a calculated spectrum assuming a shift of ω_p from 1.2055 to 1.2050 eV, upon entering the superconducting state. If we assume a "normal" temperature dependence described by Eq. (4) across T_c with the same parameters as used to produce Fig. 3(f), a T_c-induced plasma-frequency shift of 1 meV on top of the expected thermal dependence has to be used to reproduce the TDϵ_1 data. If we assume, in addition to the expected T dependence of ϵ_1 modeled by Eq. (4), a T_c-induced decrease of Γ by 2.5%, we get a plasma-frequency shift of about 3 meV. For larger changes in Γ we get lineshapes of TDϵ_1 that do not describe the experimental data.

Generally, a drop of the plasma frequency indicates that Drude-like charge carriers are removed to form the superconducting condensate. A plasma-frequency shift from 1.205 to 1.208 eV corresponds to a relative Drude-like charge-carrier loss of $\sim$0.5%, assuming that the effective mass is unchanged across the transition. This value is to be contrasted to the 10-30% estimated from data on electronic specific heat.[33] Even considering that both estimates are gross, and that condensation-energy data derived from specific-heat measurements have been shown to be reducible by a factor of 3 by subtraction of fluctuations,[34] a discrepancy of roughly one order of magnitude remains. This points towards the possibility that the superconducting condensate is not formed by Drude-like charge carriers alone, but that spectral-weight transfers from higher bands are of large importance.

In addition, the observed sudden change of ω_p cannot account for the anomalies at higher energies and not for the shape change of the TDϵ_2 spectrum either. This suggests that the high-energy optical effects observed by several groups[15–20] are not governed solely by a change of the plasma frequency, but also by other effects rooted in more local physics on energy scales of a few eV, i.e., on the magnitude of the Coulomb on-site repulsion. These simultaneous

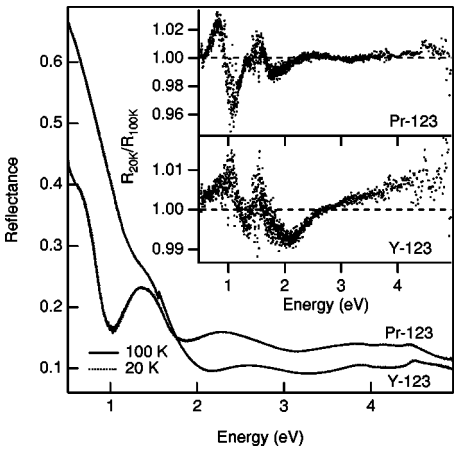

FIG. 4. Reflectances of Y-123 and Pr-123 at 100 K (slightly above T_c) and 20 K. The insets show the ratio between the low- and high-temperature reflectances.

effects on both high- and low-energy scales point directly towards the ideas about Mottness.[13,14]

For comparative purposes, we calculated the reflectances of Y-123 and Pr-123 at 100 K (slightly above T_c) and 20 K from the dielectric functions. These data can be seen in Fig. 4, and reveal that the temperature dependence of the reflectance is a weak effect in the investigated frequency range. In the insets of Fig. 4, we show the ratios between the reflectance at $T=100$ and 20 K. It is obvious from these graphs that, while the effect is twice as strong in Pr-123, the shape of the relative change of the reflectivity between these two temperatures is very similar in the two compounds. In other words, the overall changes of the reflectances are similar, in spite of the fact that the effects that can be intimately related to superconductivity in Y-123 are absent in Pr-123.

IV. CONCLUSIONS

We have determined the complex dielectric functions of Y-123 and Pr-123 thin films temperature dependently using spectroscopic ellipsometry in the spectral range from 0.5 to 5 eV. Except for the Drude-like metallic response in Y-123, we find in both compounds optical excitations at around 1.4 eV, 2.6 eV (2.3 eV for Pr-123), 2.9, 3.4, and 4.5 eV. In Pr-123 we see the 1.4-eV peak sharpen below T_N. In Y-123 we observe at low temperatures an additonal very sharp peak at 4.6 eV that cannot be resolved in the Pr-123 data.

We have investigated the data both by sum-rule analysis and thermal-difference analysis.[15,16] The sum-rule analysis shows that, while Y-123 constantly loses spectral weight from the range 0.5—5.0 eV on cooling, the total spectral weight of Pr-123 stays constant, within the experimental accuracy, from 375 K down to 20 K. It shows also that a step-wise spectral-weight transfer in Y-123 into the bands between 3.9 and 4.8 eV takes place slightly before the material enters the superconducting state. No clear sign of a similar anomaly could be seen in Pr-123.

The thermal-difference analysis gives a detailed picture of the temperature dependence of the dielectric function. Here, we showed that superconductivity-induced effects are seen

over the whole investigated spectral range in Y-123. The strong effects around 1 eV in ϵ_1 could be well described within the simple Drude model, assuming a sudden plasma-frequency decrease of the order of 0.5—3 meV when the material enters the superconducting state. It fails, however, to model the anomalies in ϵ_2, as well as the effects at energies above ~2 eV. Our results give additional evidence that high-energy correlations are important for the understanding of cuprate superconductors, as previously outlined in several studies.[15–20]

Note added. Since the submission of this work, we have learned about broad-band spectroscopic ellipsometry results from another group.[35] That work, performed on Y-123 and $Bi_2Sr_2CaCu_2O_8$, is in line with our results and provide additional evidence for the relevance of high-frequency properties.

ACKNOWLEDGMENTS

We thank U. Merkt, I. Panas, P. Phillips, T. Timusk, C. Bernhard, S. L. Cooper, and M. V. Klein for useful discussions. We acknowledge financial support of the Deutsche Forschungsgemeinschaft DFG via Ru 773/2-1, Ru 773/2-2, and Ru 773/2-3, as well as the Graduiertenkolleg Physik Nanostrukturierter Festkörper.

*Present address: Permascand AB, Box 42, SE—84010 Ljungaverk, Sweden

†Present address: Basler Vision Technologies, An der Strusbek 60–62, D-22926 Ahrensburg, Germany

[1] P. H. B. Radousky, J. Mater. Res. **7**, 1917 (1992).

[2] M. B. Maple, B. W. Lee, J. J. Neumeier, G. Nieva, L. M. Paulius, and C. L. Seaman, J. Alloys Compd. **181**, 135 (1992).

[3] R. Fehrenbacher and T. M. Rice, Phys. Rev. Lett. **70**, 3471 (1993).

[4] H. A. Blackstead and J. D. Dow, Phys. Rev. B **57**, 5048 (1998).

[5] U. Staub, M. Shi, A. G. O'Conner, M. J. Kramer, and M. Knapp, Phys. Rev. B **63**, 134522 (2001).

[6] S. S. Weng, I. P. Hong, C. F. Chang, H. L. Tsay, S. Chatterjee, H. D. Yang, and J.-Y. Lin, Phys. Rev. B **59**, 11205 (1999).

[7] H. A. Blackstead, J. D. Dow, D. B. Chrisey, J. S. Horwitz, M. A. Black, P. J. McGinn, A. E. Klunzinger, and D. B. Pulling, Phys. Rev. B **54**, 6122 (1996).

[8] K. Oka, Z. Zou, and J. Ye, Physica C **300**, 200 (1998).

[9] R. Liang, D. A. Bonn, and W. N. Hardy, Physica C **304**, 105 (1998).

[10] D. W. Cooke, R. S. Kwok, R. L. Lichti, T. R. Adams, C. Boekema, W. K. Dawson, A. Kebede, J. Schwegler, J. E. Crow, and T. Mihalisin, Phys. Rev. B **41**, 4801 (1990).

[11] D. Budelmann, S. Ostertun, M. Rübhausen, A. Bock, M. Schilling, H. Burkhardt, U. Merkt, and A. Krämer, Phys. Rev. B **63**, 174508 (2001).

[12] D. Budelmann, J. Holmlund, J. Andreasson, H. Rodríguez, J. Bäckström, L. Börjesson, H. Adrian, U. Merkt, and M. Rübhausen, Phys. Rev. B **67**, 140507 (2003).

[13] T. D. Stanescu and P. Phillips, Phys. Rev. Lett. **91**, 017002 (2003).

[14] T. D. Stanescu and P. Phillips, Phys. Rev. B **69**, 245104 (2004).

[15] M. J. Holcomb, C. L. Perry, J. P. Collman, and W. A. Little, Phys. Rev. B **53**, 6734 (1996).

[16] M. J. Holcomb, J. P. Collman, and W. A. Little, Phys. Rev. Lett. **73**, 2360 (1994).

[17] M. Rübhausen, A. Gozar, M. V. Klein, P. Guptasarma, and D. G. Hinks, Phys. Rev. B **63**, 224514 (2001).

[18] H. J. A. Molegraaf, C. Presura, D. van der Marel, P. H. Kes, and M. Li, Science **295**, 2239 (2002).

[19] I. Fugol, G. Saemann-Ischenko, V. Samovarov, Y. Rybalko, V. Zhuravlev, Y. Ströbel, B. Holzäpfel, and P. Berberich, Solid State Commun. **80**, 201 (1991).

[20] I. Fugol, V. Samovarov, A. Ratner, V. Zhuravlev, G. Saemann-Ischenko, B. Holzapfel, and O. Meyer, Solid State Commun. **86**, 385 (1993).

[21] H. L. Dewing and E. K. H. Salje, Supercond. Sci. Technol. **5**, 50 (1992).

[22] M. Rübhausen, C. T. Rieck, N. Dieckmann, K.-O. Subke, A. Bock, and U. Merkt, Phys. Rev. B **56**, 14797 (1997).

[23] R. M. A. Azzam and N. M. Bashara, *Ellipsometry And Polarized Light* (Elsevier, New York, 1999).

[24] G. Jakob, P. Przyslupski, C. Stölzel, C. Tomé-Rosa, A. Walkenkorst, M. Schmitt, and H. Adrian, Appl. Phys. Lett. **59**, 1626 (1991).

[25] K. Takenaka, Y. Imanaka, K. Tamasaku, T. Ito, and S. Uchida, Phys. Rev. B **46**, 5833 (1992).

[26] K. Widder, M. Merz, D. Berner, J. Münzel, H. P. Geserich, A. Erb, R. Flükiger, W. Widder, and H. F. Braun, Physica C **264**, 11 (1996).

[27] J. Kircher, M. K. Kelly, S. Rashkeev, M. Alouani, D. Fuchs, and M. Cardona, Phys. Rev. B **44**, 217 (1991).

[28] M. E. Bijlsma, H. Wormeester, D. H. A. Blank, E. Span, A. van Silfhout, and H. Rogalla, Phys. Rev. B **57**, 13418 (1998).

[29] M. Garriga, J. Humlíček, J. Barth, R. L. Johnson, and M. Cardona, J. Opt. Soc. Am. B **6**, 470 (1989).

[30] J. Kircher, M. Alouani, M. Garriga, P. Murugaraj, J. Maier, C. Thomsen, M. Cardona, O. K. Andersen, and O. Jepsen, Phys. Rev. B **40**, 7368 (1989).

[31] M. K. Kelly, P. Barboux, J.-M. Tarascon, D. E. Aspnes, W. A. Bonner, and P. A. Morris, Phys. Rev. B **38**, 870 (1988).

[32] D. N. Basov, R. Liang, B. Dabrowski, D. A. Bonn, W. N. Hardy, and T. Timusk, Phys. Rev. Lett. **77**, 4090 (1996).

[33] J. W. Loram, K. A. Mirza, J. R. Cooper, and W. Y. Liang, Phys. Rev. Lett. **71**, 1740 (1993).

[34] D. van der Marel, A. J. Leggett, J. W. Loram, and J. R. Kirtley, Phys. Rev. B **66**, 140501 (2002).

[35] A. V. Boris, N. N. Kovaleva, O. V. Dolgov, T. Holden, C. T. Lin, B. Keimer, and C. Bernhard, Science **304**, 708 (2004).